RESEARCH BRIEF

Genomic Characterization of Brain Metastases Reveals Branched Evolution and Potential Therapeutic Targets

Priscilla K. Brastianos[1,2,3,4,5], Scott L. Carter[5,6], Sandro Santagata[7,8], Daniel P. Cahill[9], Amaro Taylor-Weiner[5], Robert T. Jones[4,10], Eliezer M. Van Allen[4,5], Michael S. Lawrence[5], Peleg M. Horowitz[11], Kristian Cibulskis[5], Keith L. Ligon[4,8], Josep Tabernero[12,13], Joan Seoane[12,13], Elena Martinez-Saez[14], William T. Curry[9], Ian F. Dunn[11], Sun Ha Paek[15,16], Sung-Hye Park[15,16], Aaron McKenna[5], Aaron Chevalier[5], Mara Rosenberg[5], Frederick G. Barker II[9], Corey M. Gill[3], Paul Van Hummelen[4,10], Aaron R. Thorner[4,10], Bruce E. Johnson[4], Mai P. Hoang[17], Toni K. Choueiri[4], Sabina Signoretti[8], Carrie Sougnez[5], Michael S. Rabin[4], Nancy U. Lin[4], Eric P. Winer[4], Anat Stemmer-Rachamimov[17], Matthew Meyerson[4,5,8,10], Levi Garraway[4,5,6], Stacey Gabriel[5], Eric S. Lander[5], Rameen Beroukhim[4,5,7], Tracy T. Batchelor[2], José Baselga[18], David N. Louis[17], Gad Getz[3,5,17], and William C. Hahn[4,5,10]

ABSTRACT

Brain metastases are associated with a dismal prognosis. Whether brain metastases harbor distinct genetic alterations beyond those observed in primary tumors is unknown. We performed whole-exome sequencing of 86 matched brain metastases, primary tumors, and normal tissue. In all clonally related cancer samples, we observed branched evolution, where all metastatic and primary sites shared a common ancestor yet continued to evolve independently. In 53% of cases, we found potentially clinically informative alterations in the brain metastases not detected in the matched primary-tumor sample. In contrast, spatially and temporally separated brain metastasis sites were genetically homogenous. Distal extracranial and regional lymph node metastases were highly divergent from brain metastases. We detected alterations associated with sensitivity to PI3K/AKT/mTOR, CDK, and HER2/EGFR inhibitors in the brain metastases. Genomic analysis of brain metastases provides an opportunity to identify potentially clinically informative alterations not detected in clinically sampled primary tumors, regional lymph nodes, or extracranial metastases.

SIGNIFICANCE: Decisions for individualized therapies in patients with brain metastasis are often made from primary-tumor biopsies. We demonstrate that clinically actionable alterations present in brain metastases are frequently not detected in primary biopsies, suggesting that sequencing of primary biopsies alone may miss a substantial number of opportunities for targeted therapy. *Cancer Discov; 5(11); 1–13. ©2015 AACR.*

[1]Department of Medicine, Massachusetts General Hospital, Harvard Medical School, Boston, Massachusetts. [2]Department of Neurology, Massachusetts General Hospital, Harvard Medical School, Boston, Massachusetts. [3]Cancer Center, Massachusetts General Hospital, Harvard Medical School, Boston, Massachusetts. [4]Department of Medical Oncology, Dana-Farber Cancer Institute, Boston, Massachusetts. [5]Broad Institute, Boston, Massachusetts. [6]Joint Center for Cancer Precision Medicine, Dana-Farber Cancer Institute, Boston, Massachusetts. [7]Department of Cancer Biology, Dana-Farber Cancer Institute, Boston, Massachusetts. [8]Department of Pathology, Brigham and Women's Hospital, Harvard Medical School, Boston, Massachusetts. [9]Department of Neurosurgery, Massachusetts General Hospital, Harvard Medical School, Boston, Massachusetts. [10]Center for Cancer Genome Discovery, Dana-Farber Cancer Institute, Boston, Massachusetts. [11]Department of Neurosurgery, Brigham and Women's Hospital, Harvard Medical School, Boston, Massachusetts. [12]Department of Medical Oncology, Vall d'Hebron University, Barcelona, Spain. [13]Department of Pathology, Vall d'Hebron University, Barcelona, Spain. [14]Vall d'Hebron University Hospital and Institute of Oncology (VHIO), Barcelona, Spain. [15]Department of Neurosurgery, Seoul National University College of Medicine, Seoul, South Korea. [16]Department of Pathology, Seoul National University College of Medicine, Seoul, South Korea. [17]Department of Pathology, Massachusetts General Hospital, Harvard Medical School, Boston, Massachusetts. [18]Department of Medicine, Memorial Sloan Kettering Cancer Center, New York, New York.

Note: Supplementary data for this article are available at Cancer Discovery Online (http://cancerdiscovery.aacrjournals.org/).

P.K. Brastianos and S.L. Carter contributed equally to this article. G. Getz and W.C. Hahn contributed equally to this article.

doi: 10.1158/2159-8290.CD-15-0369

INTRODUCTION

Brain metastases, most frequently originating from melanoma and carcinomas of the lung and breast, are the most common tumor in the brain. Approximately 200,000 cases are diagnosed annually in the United States alone. Patients frequently develop brain metastases even while their extracranial disease remains under control (1). Median survival ranges from 3 to 27 months following metastatic spread to the brain (1). Of patients who have clinically symptomatic brain metastases, approximately half succumb to the cancer in their brain (2). Unfortunately, treatment options are limited, and most current clinical trials in the United States exclude patients with brain metastases.

Because cancers are genetically heterogeneous (3–9), sampling a cancer in two different locations is expected to reveal mutations exclusive to each sample. Furthermore, because brain metastases are often resected during clinical care, such tissue provides an immediate opportunity for genomic assessment of these life-threatening lesions. To date, the extent to which brain metastases, often manifesting years after the primary malignancy, share the genetic profile of the primary tumor remains unknown. Massively parallel sequencing of brain metastases has been performed on a limited number of cases (7, 10), showing novel alterations in the metastatic site. Prior studies have suggested activation of the PI3K pathway in brain metastases (11, 12). Some gene expression signatures have been associated with metastasis to the brain (13, 14).

We performed whole-exome sequencing on 86 "trios" of patient-matched brain metastases, primary tumors, and normal samples, all of which were collected in the course of clinical care (e.g., for diagnosis, symptom control, or restaging). For 15 patients, we also characterized multiple metastatic brain lesions, distal extracranial metastases, and additional samples from the primary tumor or associated regional lymph nodes. Our objectives were to (i) determine whether clinically sampled brain metastases harbor distinct potentially clinically informative mutations not detected in paired primary-tumor samples; (ii) determine the extent to which such mutations are shared among multiple regions of a single brain metastasis, anatomically distinct brain metastasis sites, and temporally separated lesions (in cases that recurred following therapy); and (iii) determine whether lymph nodes or extracranial metastases are genetically similar to brain metastases and might serve as their proxy for genomic assessment and clinical decision making.

Current affiliations for S.L. Carter: Joint Center for Cancer Precision Medicine, Dana-Farber Cancer Institute, Brigham and Women's Hospital, Broad Institute of Harvard and MIT, Harvard Medical School, Boston, Massachusetts; Department of Biostatistics and Computational Biology, Dana-Farber Cancer Institute, Boston, Massachusetts; Department of Biostatistics, Harvard School of Public Health, Boston, Massachusetts; Broad Institute of Harvard-MIT, Boston, Massachusetts.

Corresponding Authors: Priscilla K. Brastianos, Division of Neuro-Oncology, Massachusetts General Hospital, 55 Fruit Street, Yawkey 9E, Boston, MA 02114. Phone: 617-643-1938; Fax: 617-643-2591; E-mail: pbrastianos@partners.org; William C. Hahn, Department of Medical Oncology, Dana-Farber Cancer Institute, 450 Brookline Avenue, Dana 1538, Boston, MA 02215. Phone: 617-632-2641; E-mail: william_hahn@dfci.harvard.edu; Scott L. Carter, Cancer Program, Broad Institute of Harvard and MIT, 415 Main Street, Cambridge, MA 02142. Phone: 617-714-7571; E-mail: carter.scott@jimmy.harvard.edu; and Gad Getz, Cancer Program, Broad Institute of Harvard and MIT, 415 Main Street, Cambridge, MA 02142. Phone: 617-714-7471; E-mail: gadgetz@broadinstitute.org

RESULTS

Patients

Clinical characteristics of the 86-patient case series are shown in Supplementary Table S1. The majority of the cases were derived from lung ($n = 38$), breast ($n = 21$), and renal cell carcinomas ($n = 10$). Of the 86 patients, 48 had a single brain metastasis, whereas the rest of the cases had additional brain metastases diagnosed radiographically.

Genetic Divergence of Brain Metastases and Primary Tumors

Several lines of evidence indicate that tumors exhibit genetic heterogeneity both across different anatomic regions (3–6, 8, 15) and within single cancer-tissue samples (7, 9, 16, 17). We applied previously described computational methods to address the heterogeneity of cancer-tissue samples and inferred the evolutionary relationship between the sequenced tissue samples from each patient (16, 18–20). We integrated data from somatic point mutations and copy-number alterations to estimate the fraction of cancer cells harboring each point mutation; that is, their cancer-cell fraction (CCF; refs. 16, 18–21). Analysis of the CCF for each mutation across the tissue samples derived from the same patient allowed us to infer phylogenetic trees relating all cancer subclones detected (Supplementary Figs. S1–S6).

Corroborating prior observations, all clonally related primary tumor and brain metastasis samples were consistent with a branched evolution pattern (4, 22). Although they shared a common ancestor, both the primary tumor and the metastasis continued to evolve separately, reflected by (i) the presence of distinct mutations ("private mutations") with a CCF = 1 (i.e., present in all cancer cells) in both samples (Supplementary Figs. S1 and S7); and (ii) the fact that each sample continued to develop minor cancer-cell populations defined by mutations with CCF < 1.

We failed to identify a minor cancer-cell population in any primary-tumor sample that was the ancestor of its paired metastasis. Such a metastasis-founding subclone would harbor mutations in a subset of the cancer cells of the primary-tumor sample ($CCF_{primary} < 1$) that were present in all cancer cells ($CCF_{met} = 1$) of the metastasis sample (Supplementary Fig. S7B). Although it is possible that more comprehensive sampling of primary-tumor tissue might have revealed such founding ancestor subclones (20, 22), this would not have been clinically feasible in most cases.

In four of 86 primary/metastasis pairs analyzed, we did not identify common mutations between the primary tumor and metastasis samples, suggesting that they were clonally unrelated (Supplementary Fig. S7C). Three of these arose in the lungs of smokers, with multiple histologically distinct primary tumors diagnosed clinically. An additional patient with breast cancer had another primary tumor in the contralateral breast; this patient was found to harbor a heterozygous germline *BRCA1* (5385insC) allele. These 4 patients likely developed

multiple clonally independent cancers in the context of exposure to tobacco carcinogens or germline risk, suggesting that their brain metastases arose from separate primary tumors (unavailable for analysis).

In many cases, we identified potentially clinically relevant mutations in the brain metastasis that were not detected in the clinically sampled primary tumor. Because the primary and metastatic tissue samples were fully diverged siblings with no detectable overlap of subclones, we calculated power to have observed these mutations in the primary-tumor samples assuming a CCF of 1.0. However, it could be argued that small subclones representing ancestors of the metastasis might have been present in the primary samples, but not detected (because their CCF would not significantly displace that of their sibling subclones with apparent CCF = 1.0 in the primary sample). We therefore also calculated the minimum CCF of these mutations in the primary sample for which we had detection power ≥ 0.95 (minimum CCF_{95}).

For example, in a patient who had undergone resection of a primary renal cell carcinoma (case 218), but subsequently developed both extracranial metastases 3 years after resection and a brain metastasis 7 months later while on bevacizumab for progressive extracranial disease, we detected a homozygous *PTEN* nonsense mutation in the brain metastasis, but not in the primary-tumor sample. Biallelic loss of *PTEN* may correlate with sensitivity to some PI3K/AKT/mTOR inhibitors (23), and has also been found to mediate resistance to other inhibitors, including EGFR (24) and PI3K inhibitors (25). Deep sequencing of the primary-tumor sample using an independent library further supported the absence of the mutation (0 of 263 reads; power > 0.99; minimum CCF_{95} = 0.032). As previously reported in non–central nervous system metastases of clear-cell renal cell carcinoma (ccRCC; ref. 4), we also observed convergent evolution in this case, with distinct *PBRM1* frameshift mutations present in the brain metastasis and primary tumor, confirmed with deep sequencing of the primary tumor (Fig. 1A and Supplementary Table S2).

A second patient (24) with a single synchronous brain metastasis from ccRCC had mutations in *MTOR*, *VHL*, and *PBRM1* that were shared by the metastasis and primary tumor. Additional alterations in *PIK3CA* (p.E542K) and *CDKN2A* (homozygous deletion) were detected only in the brain-metastasis sample (Fig. 1B and Supplementary Fig. S8). Deep sequencing with an independent library failed to detect *PIK3CA* (Supplementary Table S2) in the primary-tumor sample (0 of 733 reads, power > 0.99; minimum CCF_{95} = 0.014).

A third patient (135) with HER2-amplified breast cancer and stable extracranial disease developed a brain metastasis after 3 years of trastuzumab therapy. The brain metastasis and primary tumor shared an amplification in *ERBB2* and a homozygous deletion of *TP53*; however, the primary tumor harbored an additional *MYC* amplification that was not observed in the brain-metastasis sample, and the brain metastasis harbored a homozygous missense mutation of uncertain significance in *BRCA2* (p.H2563N) that was not detected in the primary-tumor sample (0/82 reads; Fig. 1C). Deep sequencing of an independent library from the primary-tumor sample (0/133 reads; power > 0.99; minimum CCF_{95} = 0.027) also failed to detect the *BRCA2* mutation (Supplementary Table S2).

A fourth patient (0244) with HER2-amplified breast cancer developed a brain metastasis after 2 years of trastuzumab therapy. We detected both a broad amplification (six copies) and an activating point mutation in *EGFR* (L858R; 7/129 reads) in the metastasis sample. In this case, the mutant L858R allele was not amplified, consistent with the amplification having occurred prior to the mutation (Fig. 1D). Both the amplification and the mutation were not observed in the primary-tumor sample (0/204 reads; Fig. 1D) validated with additional deep sequencing (0/419 reads; power > 0.99, minimum CCF = 0.067; Supplementary Table S2). Although the L858R mutation is common in lung cancers and is associated with sensitivity to gefitinib (26), one proposed mechanism of resistance in anti-HER2 therapy in breast cancer is activation of EGFR (27, 28), suggesting that trastuzumab therapy may have selected for this mutant allele. We also detected an *FGFR1* amplification in the brain metastasis and a *CCND2* amplification in the primary tumor (Fig. 1D).

A fifth patient (331) with serous ovarian cancer experienced a complete remission for 1 year following chemotherapy and subsequently developed a solitary brain metastasis 5 years later. The brain metastasis harbored a high-level amplification of *ERBB2* (32 copies). Using immunohistochemical staining, we confirmed that HER2 was indeed overexpressed in the metastasis and was not detected in the primary tumor sample (Fig. 1E). Although *HER2* amplifications are not commonly observed in serous ovarian cancer (29), such amplification events have been shown to confer sensitivity to anti-HER2 therapy in breast and other cancers (30). We also identified a *BRAF* amplification in the primary tumor that was not present in the brain-metastasis sample (Fig. 1E). Further amplifications of *FGFR1* and *MYC* were detected only in the brain metastasis (6 and 7 copies, respectively; Supplementary Fig. S9). These five examples demonstrate that genomic sampling of resected brain metastases revealed potentially actionable mutations not detected in the clinically sampled primary tumors.

The Landscape of Clinically Informative Driver Alterations in Clinically Sampled Brain Metastases and Primary Tumors

The genetic divergence observed between clinically sampled primary tumors and brain metastases implies that potentially clinically actionable targets present in the brain metastasis may not be detected from analysis of a single sample of the primary tumor (Fig. 1 and Supplementary Fig. S1). We therefore evaluated the extent to which primary-tumor biopsies and resected brain metastases, collected as part of clinical care, would allow identification of oncogenic alterations with potential clinical significance across our entire series of 86 paired cases. To systematically perform this evaluation, we used the TARGET database (31) of genes for which somatic alterations have therapeutic or prognostic implications (Supplementary Table S3). Many of the TARGET alterations serve as eligibility criteria in the context of genomically guided clinical trials in cancer, both histology specific or independent of histology (31). Alterations in TARGET genes were

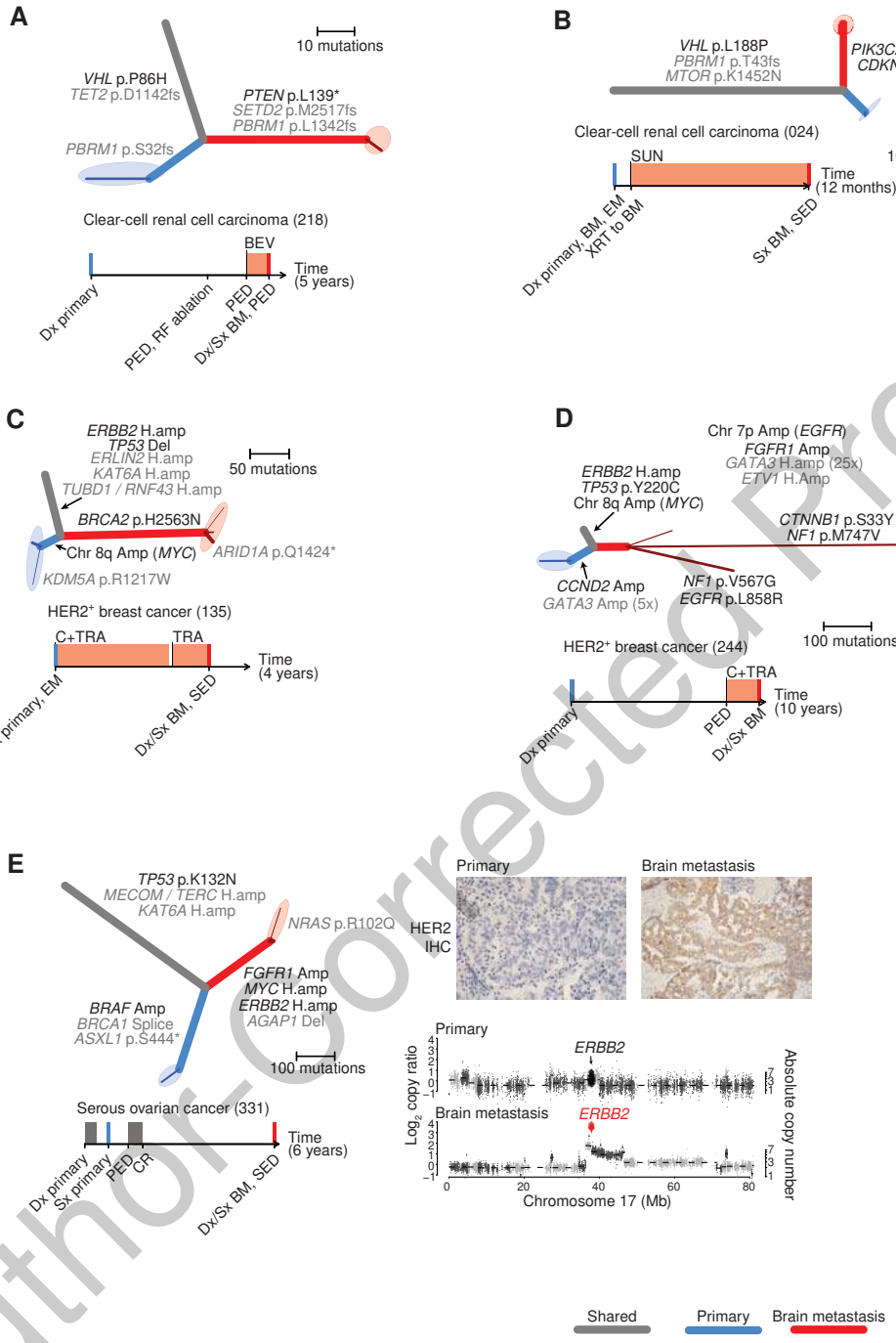

Figure 1. Brain metastases harbor clinically actionable mutations not detected in primary-tumor samples. **A–E,** phylogenetic trees inferred for five example cases. Branch colors indicate the types of tissue samples descended from each branch (gray, shared by all samples; blue, primary-tumor sample; red, brain metastasis). Darker-colored lines correspond to subpopulations of cancer cells detected with CCF < 1; the maximally branching evolutionary relationships of these clusters are drawn on the ends of each sample branch, surrounded by shaded ellipses denoting the tissue sample. The thickness of each branch is proportional to the CCF of mutations on that branch. Potentially clinically informative (TARGET) alterations (black) and additional likely oncogenic alterations (gray) are annotated onto the phylogenetic branches on which they occurred. Timelines depict the sequence of diagnosis, treatment, and tissue sampling for each case, with chemotherapy treatment intervals denoted by gray rectangles, and treatment with specified targeted agents denoted by orange rectangles. Colored vertical lines denote collection of sequenced cancer tissues (blue, primary; red, brain metastasis). BEV, bevacizumab; BM, brain metastasis; BM1, brain metastasis from one anatomic location; BM2, brain metastasis from second anatomic location; Bx, biopsy; C, chemotherapy; CET, cetuximab; CR, complete response; Dx, diagnosis; EM, extracranial metastasis; I-131, radioactive iodine; LAP, lapatinib; LN, lymph node; PARPi, PARP inhibitor; PBM, progressive brain metastasis; PED, progressive extracranial disease; PI3Ki, PI3K inhibitor; SED, stable extracranial disease; Sx, surgery; SUN, sunitinib; TRA, trastuzumab; WBRT, whole brain radiotherapy; XRT, radiation. **E,** also shows immunohistochemical staining (IHC) for HER2 in samples of the primary tumor (left), and brain metastasis (right). In addition, genomic copy ratios on chromosome 17 are shown (bottom) for the primary-tumor sample (top) and brain metastasis (bottom). Large diamonds correspond to exons of *ERBB2*, colored according to amplification status (black, unamplified; red, amplified).

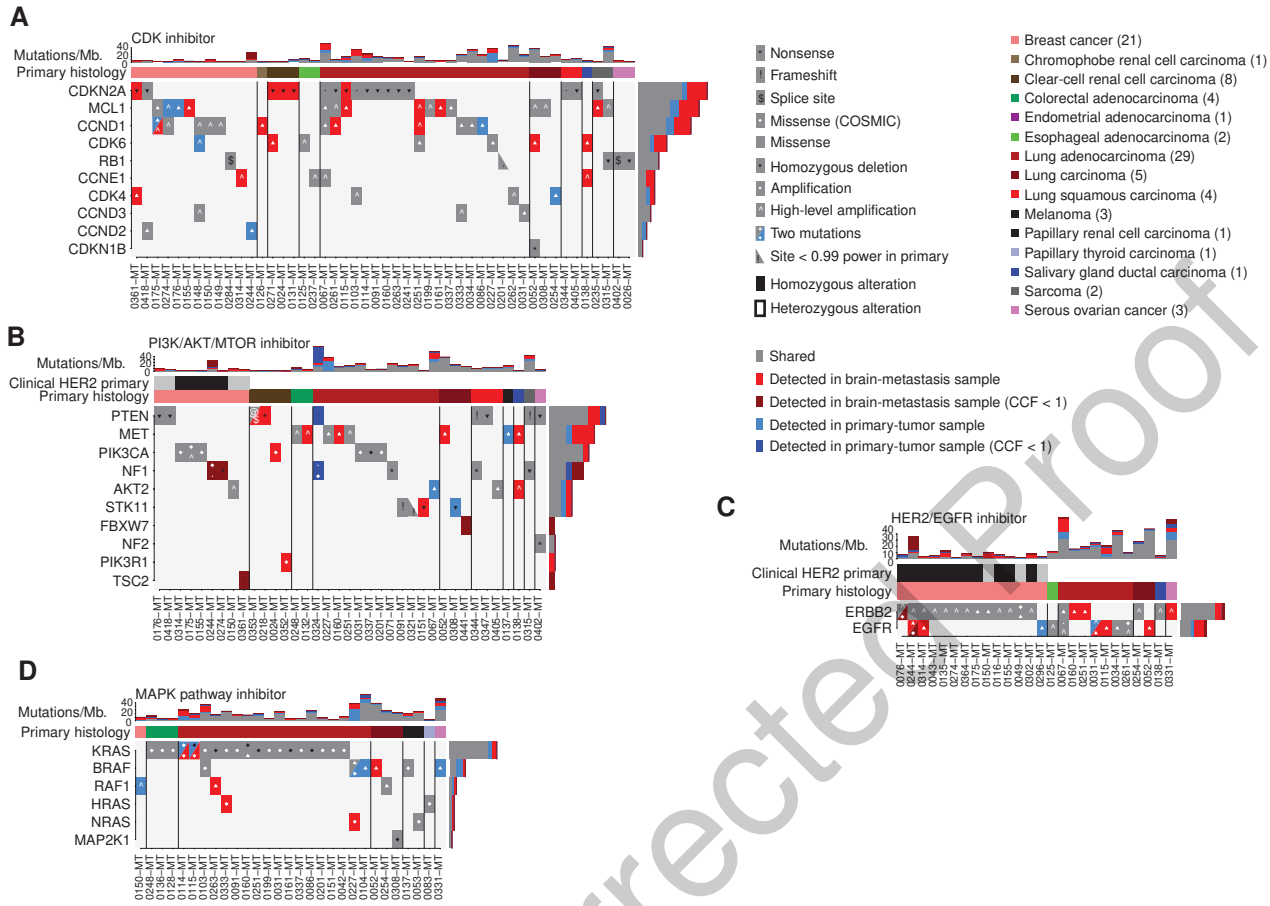

Figure 2. The landscape of potentially clinically actionable alterations in brain metastases and primary-tumor samples. **A–D,** alterations in genes (rows) that may predict sensitivity to the indicated class of targeted agent. Vertical columns correspond to cases, which are ordered by primary histology and presence/absence of alterations. Stacked bar graphs indicating the number of somatic point mutations detected in each phylogenetic branch of each case (columns) are shown at the top of each panel. HER2 status determined during clinical evaluation is denoted by: black, positive; gray, negative; white, not measured. COSMIC, Catalogue of Somatic Mutations in Cancer.

prioritized according to defined criteria (31). For example, some genes were required to have biallelic inactivation, whereas others required amplification or specific point mutations. To organize our analysis, we partitioned the TARGET genes into 13 categories (Supplementary Table S3) corresponding to alterations that may be associated with response to specific classes of targeted therapies, or which consist of important cancer drivers associated with prognosis (Fig. 2 and Supplementary Fig. S10).

A total of 95,431 gene alterations were detected across our dataset, of which 330 met the TARGET criteria of being clinically informative. Forty-six of 86 (53%) cases harbored at least one such potentially actionable alteration in the brain metastasis that was not identified in the paired primary-tumor sample. For all mutations detected exclusively in either the primary tumor or metastasis sample of a given patient, we confirmed that sequencing depth covering the absent mutation provided adequate detection power (>0.99; Supplementary Fig. S11).

Alterations potentially predicting sensitivity to cyclin-dependent kinase (CDK) inhibitors (31–33) were common across our case series, with 71 alterations in 48 cases occurring in 10 of 11 evaluated genes (Fig. 2A). Of the 71 alterations, 44 were shared, seven were only in the primary sample, and 20 were only in the brain-metastasis sample. The most frequently altered gene in this group was *CDKN2A*, with 17 events in total, including homozygous deletions in three of eight ccRCC cases that were only in the brain-metastasis samples (Fig. 2A). *MCL1* amplifications, which preclinical studies have shown to be associated with sensitivity to CDK inhibitors (34), were also common; five out of the 15 events were detected only in the brain-metastasis samples. In addition, five cases had shared homozygous *RB1* loss, which is associated with resistance to CDK inhibitors (35).

Mutations affecting the PI3K–AKT–mTOR pathway were also frequent, with 43 alterations in 37 cases occurring in 10 of 15 evaluated genes (Fig. 2B). Of the 43 alterations, 24 were shared, five were detected only in the primary samples, and 14 were detected only in the brain-metastasis samples. Actionable alterations in these genes occurred frequently in breast cancers (9/21 cases, 6/9 of which were shared), and lung adenocarcinoma (12/29 cases, 8/12 of which were shared). Four of the eight brain metastases from patients with primary ccRCC harbored mutations in the

PI3K–mTOR pathway detected only in the brain-metastasis samples. In addition to the *PTEN* mutation described above (Fig. 1A), another case had a shared small in-frame deletion (p.D52del) in *PTEN* with an additional splice site mutation detected only in the brain-metastasis sample. A third ccRCC case harbored a *PIK3CA* E542K mutation (Fig. 1B and Fig. 2B), and a fourth harbored a *PIK3R1* N564D mutation previously reported in glioblastoma (36) that activates the PI3K–AKT pathway (37). A fifth ccRCC brain metastasis harbored a small frameshift deletion in *PTEN* (K6fs) that was predicted to be heterozygous (not shown). Activation of the PI3K–mTOR pathway has been reported in metastatic ccRCC lesions in extracranial sites (4).

We also found mutations that predict sensitivity to HER2/EGFR inhibitors (e.g., trastuzumab, gefitinib, cetuximab, erlotinib, lapatinib) in 26 cases in two of four evaluated genes (32 alterations, 20 shared, 2 only in primary-tumor samples, 10 only in brain-metastasis samples). Thirteen of 21 breast cancers harbored amplifications in *ERBB2*, all of which were shared. In one case (076), we detected an additional activating *ERBB2* missense mutation (V777L; ref. 38) only in the brain-metastasis sample in addition to the shared *ERBB2* amplification. Notably, 2 patients with lung cancer (Fig. 2C) and a third with ovarian cancer (Fig. 1E) had *ERBB2* amplifications detected only in the brain-metastasis samples. Two patients with HER2-amplified breast cancer harbored *EGFR* alterations detected only in the brain-metastasis samples; in addition to the case above (Fig. 1E), a second patient harbored broad amplification of *EGFR* (seven copies; Fig. 2C).

The MAPK pathway inhibitor family includes agents that inhibit *BRAF* and *MEK* , such as vemurafenib, dabrafenib, or trametinib (31). Thirty-six alterations associated with response to these agents were detected in 29 cases, in 6 of 11 evaluated genes (24 shared, 6 only in the primary samples, 6 only in the brain-metastasis samples; Fig. 2D). Activating mutations in *KRAS*, which have been associated with tumor responses to MEK inhibitors (39, 40), were the most frequent alteration in this group (19 cases) and were shared in all clonally related cases.

Additional alterations under investigation for association with various targeted therapies, including Ephrin inhibitors, epigenetic therapy, Notch inhibitors, WNT inhibitors, AURKA inhibitors, multitargeted tyrosine kinase inhibitors, MDM inhibitors, PARP inhibitors, as well as alterations that might be diagnostic or prognostic, are shown in Supplementary Fig. S10.

Genetic Homogeneity of Brain Metastases

The discrepancy in the oncogenic alterations detected in clinically obtained samples from the primary tumors and matched brain metastases raised the possibility that every distinct brain metastasis lesion might harbor a unique set of oncogenic alterations. Therefore, we sought to evaluate the extent to which clinical sampling of a single brain metastasis region might be representative of the genetic alterations detected across various sites of intracranial metastasis (Fig. 3A–G). We assessed intralesion heterogeneity (by sampling multiple regions of single brain metastases), as well as interlesion heterogeneity (by sampling from multiple anatomically and temporally distinct brain metastases in the same patient). In each scenario, we observed that all profiled brain-metastasis samples shared mutations that were not detected in the clinically sampled primary tumor, indicating that the subclones sampled in these lesions were more related to one another than to those detected in the primary-tumor sample (Fig. 3A–G). Most importantly, the brain metastases shared nearly all of the potentially clinically informative driver alterations (29 of 30 alterations in 7 samples; Fig. 3A–G).

For four cases (Fig. 3A–C, and G; 0302, 0308, 0314, 0137), we analyzed multiple regions of the same brain metastasis resection. In one example case (0314), we sampled four distinct regions of a cerebellar metastasis from a patient with metastatic HER2-amplified breast cancer (Fig. 3C; 314) and found that each of these metastatic sites shared a *PIK3CA* mutation (E542K) and an amplification of *ERBB2* with the primary tumor. In addition, we found *CCNE1* and *EGFR* amplifications in all of the metastatic brain lesions that were not detected in the primary-tumor sample (Supplementary Figs. S12 and S13). The patient ultimately received treatment with a PI3K inhibitor, with no evidence of intracranial disease progression for 8 months.

For four cases (Fig. 3B, D, E, and G; 0308, 0098, 0176, 0137), we obtained and analyzed samples from brain metastases taken prior to treatment and again at the time of recurrence. For example, in a patient with a large cell neuroendocrine lung cancer (0308; Fig. 3B), we sequenced resections of brain metastases before and following whole-brain radiation and found that each sample shared a *MYC* amplification (six copies) that was not detected in the primary-tumor sample (Fig. 3B and Supplementary Fig. S14). In another example, a patient with an estrogen receptor–, progesterone receptor–, and HER2-negative (triple-negative) breast cancer (Fig. 3E; 0176) underwent a resection for a symptomatic cerebellar metastasis, and 2 months later had a rapid local recurrence, necessitating reresection (Fig. 3E). The primary tumor and brain metastases shared alterations in *TP53*, *PTEN*, and *MYC*. The primary tumor harbored an *MCL1* amplification that was not detected in the brain-metastasis samples. We also identified an additional mutation in *EZH2* (p.N640S; refs. 31, 41) in both brain metastases but failed to detect this mutation in the primary-tumor sample.

In two cases where anatomically distinct brain metastases were resected, we found that they were closely related to one another and harbored identical potentially clinically informative alterations (Fig. 3F and G). For example, a patient with a *HER2*-amplified salivary gland ductal carcinoma (Fig. 3F; 0138) developed brain metastases while being treated with trastuzumab. Analysis of a resected approximately 2 cm^3 cerebellar metastasis revealed potentially clinically informative amplifications, including *MET, CDK6*, *CCNE1*, *MYC*, and *AKT2*, that were not identified in the primary-tumor sample (Supplementary Figs. S15–S17). Ten months later, following whole-brain radiation, the patient underwent a resection of a symptomatic parietal lobe metastasis, which shared the same amplifications. Notably, at the time of progression in both brain metastases, there was no evidence of extracranial disease, and biopsy of an extracranial site for genetic analysis would not have been possible.

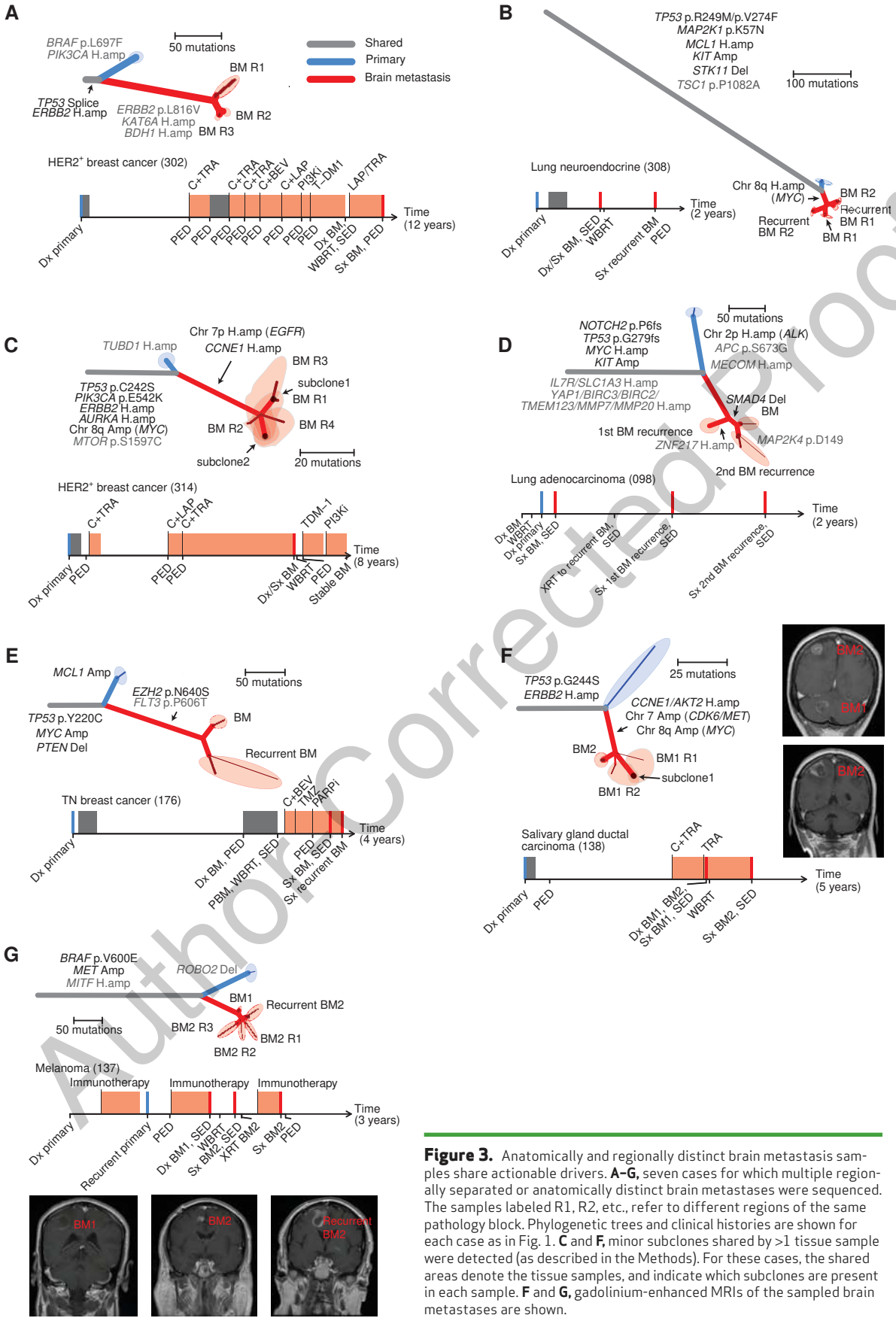

Figure 3. Anatomically and regionally distinct brain metastasis samples share actionable drivers. **A–G,** seven cases for which multiple regionally separated or anatomically distinct brain metastases were sequenced. The samples labeled R1, R2, etc., refer to different regions of the same pathology block. Phylogenetic trees and clinical histories are shown for each case as in Fig. 1. **C** and **F,** minor subclones shared by >1 tissue sample were detected (as described in the Methods). For these cases, the shared areas denote the tissue samples, and indicate which subclones are present in each sample. **F** and **G,** gadolinium-enhanced MRIs of the sampled brain metastases are shown.

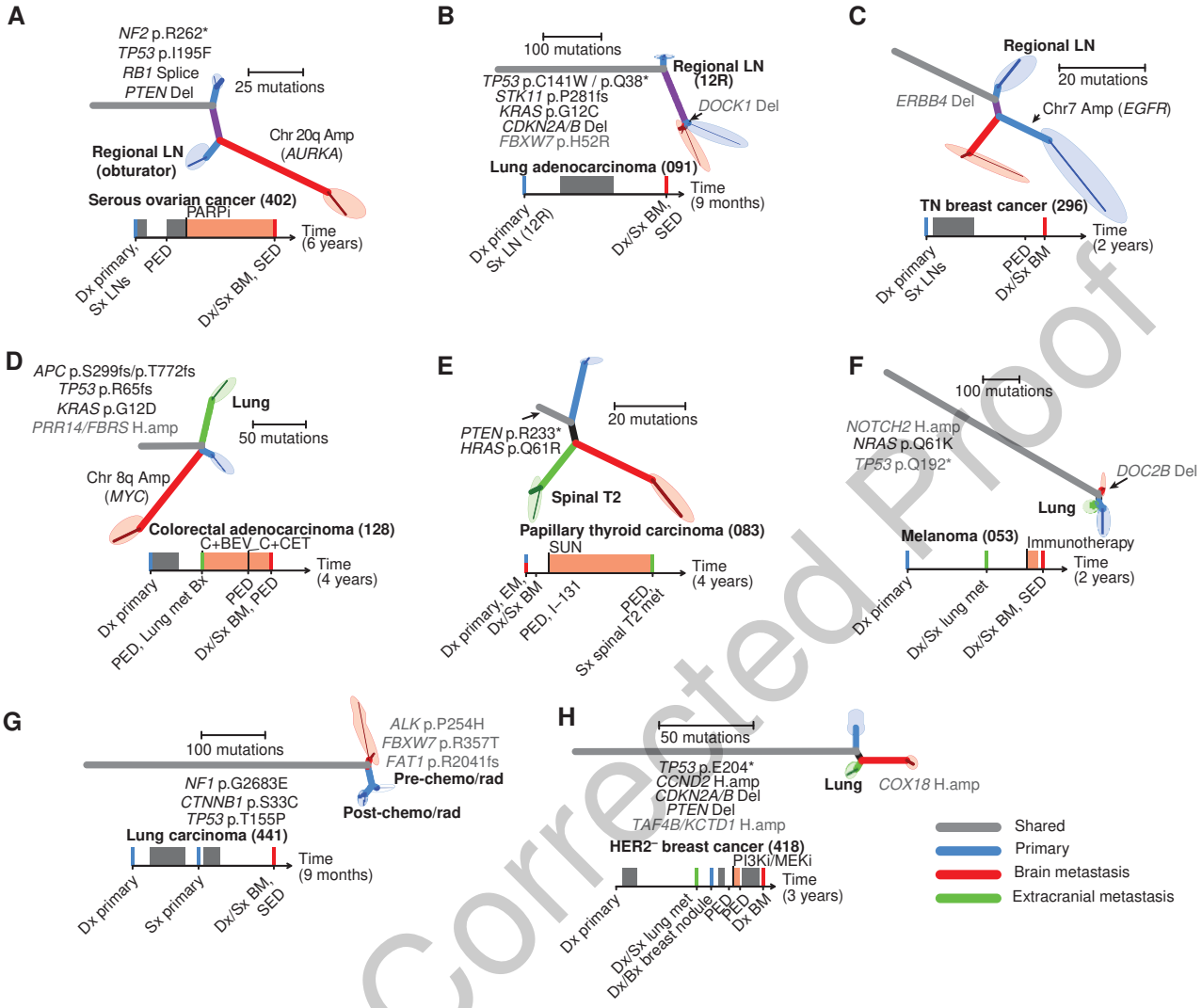

Figure 4. Regional lymph nodes and distal extracranial metastases are not a reliable surrogate for actionable mutation in brain metastases. **A–H,** 8 cases for which at least one primary tumor sample, regional lymph node, and extracranial metastasis were sequenced. Phylogenetic trees and clinical histories are shown for each case as in Fig. 1. Tissue samples from extracranial metastases are depicted in green.

Brain Metastases Are Genetically Distinct from Regional Lymph Nodes and Extracranial Metastases

Given that brain metastases can be clinically difficult to access in some cases, we evaluated the extent to which regional lymph nodes and distal extracranial metastases were genetically similar to the brain metastases. We sequenced eight cases with at least one additional primary-tumor sample, regional lymph node, or extracranial metastasis, in addition to the paired brain metastasis (Fig. 4A–G).

The extracranial sites exhibited varying degrees of relatedness to the primary tumor and brain-metastasis samples. In four of eight cases, the number of mutations private to the brain metastasis sample was greater than the number of truncal mutations shared by all samples (Fig. 4A, C, D, and E; 402, 296, 128, 83). Notably, in case 296, broad amplification of chromosome 7 (six copies), including the *EGFR* locus, was detected in the primary-tumor sample, but not in matched samples from a regional lymph node or brain metastasis (Fig. 4C and Supplementary Fig. S18).

In 2 of 4 patients with distal extracranial metastases, the metastatic sites each harbored an approximately equal or greater number of private mutations than the number of mutations that were shared (truncal) or private to the brain-metastasis sample (Fig. 4D and E; 0128, 0083). In the third case, the clinically sampled primary tumor and lung metastasis shared a common ancestor that harbored mutations not detected in the brain-metastasis sample (Fig. 4F; 053). In the fourth case, the brain and lung metastases shared a common ancestor not in common with the primary-tumor sample; however, the brain metastasis had more private mutations than the primary and lung metastasis combined (Fig. 4H; 0418).

In case 441, we sampled two regions of a primary lung carcinoma, one before and one after two cycles of neoadjuvant

chemotherapy and chest radiation, in addition to a brain metastasis that was diagnosed 5 months later in the absence of any extracranial disease (Fig. 4G). The two samples from the primary tumor shared mutations that were not detected in the brain-metastasis sample, and the brain metastasis harbored mutations of uncertain significance in *ALK* (P254H), *FBXW7* (R357T), and *FAT1* (R2041fs) that were not detected in either primary-tumor samples (Fig. 4G).

DISCUSSION

Brain metastases represent an unmet need in current oncologic care. Approximately 8% to 10% of patients with cancer will develop brain metastases, and more than half of these patients will die within a few months following diagnosis of intracranial metastasis (1). Genomically guided clinical trials have been successful at matching patients to novel targeted agents in patients with advanced cancer; however, patients with active brain metastases are routinely excluded from these trials in part due to the poor correlation between systemic response and brain response (1). Patients will often develop progressive brain metastases in the setting of extracranial disease that is adequately controlled with existing chemotherapies or targeted therapies. Historically, this clinical divergence has been ascribed to inadequate systemic therapeutic penetration of the blood–brain barrier. The observations presented here suggest that additional potentially oncogenic alterations may be present in brain metastases, and might contribute to this divergence of therapeutic response in some of these cases.

We note that these mutations may represent precursors in the evolutionary process leading to the metastasis; for example, they may have driven the proliferation or survival of a prometastatic subclone within the primary tumor (that was not sampled clinically). Alternately, it is possible that some of these alterations were necessary for the establishment of the initial metastatic outgrowth in the brain, but not for its continued growth or maintenance. In addition, we note that it is possible that some of the dependencies associated with these alterations may be histology specific or dependent on the presence or absence of additional mutations. As our study involved a retrospective collection of samples, further prospective clinical studies with agents that cross the blood–brain barrier will be required to demonstrate that these mutations are viable therapeutic targets for patients with brain metastases.

We found that 46 of 86 (53%) patients harbored a potentially clinically actionable alteration in the brain metastasis that was not detected in the clinically sampled primary tumor (Fig. 2). These alterations may have critical clinical implications because (i) patients often develop brain metastases even when presumably truncal mutations identified in the primary tumor are successfully targeted with active systemic agents [e.g., BRAF inhibitors (42), ALK inhibitors (43), or HER2 inhibitors (44)]; (ii) additional evolution in the brain metastasis lineage might contribute to treatment resistance; (iii) actionable mutations present in the brain metastasis cannot be reliably identified on the basis of only a single biopsy of the primary tumor (Fig. 2); and (iv) the primary and metastatic cancer samples may be clonally unrelated, as was the case in four of the 86 cases in our study. Because more than 50% of patients with brain metastases will die of intracranial progression, targetable alterations present in cancer subclones specific to the brain metastasis represent an important opportunity for novel targeted therapeutic strategies to affect overall survival.

Tissue from craniotomies provides an immediate opportunity for more informed decision-making based on genomic analysis. Many patients will have a brain metastasis resected as part of clinical care. Current clinical indications for craniotomies in brain metastases include: need for histologic diagnosis; resection of single (25%–50% of brain metastases; refs. 45–47) or oligometastatic disease in the setting of controlled extracranial disease; or resection of a symptomatic or dominant lesion in the setting of multiple brain metastases. Here, we show that although genetically divergent from samples of their primary tumor (Figs. 1 and 2), intracranial metastases were remarkably homogenous with respect to driver and/or potentially targetable alterations (Fig. 3), a finding with implications for the metastatic tropism of evolutionary branches that arise early during neoplastic development. Practically, this homogeneity implies that, when clinically available, characterization of even a single brain metastasis lesion may be more informative than that of a single primary tumor biopsy for selection of a targeted therapeutic agent. Notably, regional lymph node and distal extracranial metastases were not reliable surrogates for the oncogenic alterations found in brain metastases (Fig. 4).

We note that more comprehensive characterization of the primary tumor might reveal subclones that more closely resemble intracranial disease. In current clinical practice, however, decisions are often made after bulk molecular analysis of only a single biopsy from the primary tumor; without a sample of brain metastasis tissue it is impossible to determine to what extent genetic alterations in the primary biopsy represent the divergent evolutionary branch of brain metastases. In future studies, analysis of circulating tumor cells or cell-free DNA (from either blood or cerebrospinal fluid) should be assessed in the context of existing brain-metastasis tissue and autopsy studies in order to establish to what extent they might be informative regarding actionable genomic alterations in brain metastases.

METHODS

The study was reviewed and approved by the human subjects Institutional Review Boards of the Dana-Farber Cancer Institute (Boston, MA), Brigham and Women's Hospital (Boston, MA), Broad Institute of Harvard and MIT (Boston, MA), Massachusetts General Hospital (Boston, MA), Seoul National University College of Medicine (Seoul, South Korea), and Vall d'Hebron University Hospital (Barcelona, Spain). The study was conducted in accordance with the Declaration of Helsinki. Written informed consent was obtained from all participants. We identified 104 matched brain metastases, primary tumors, and normal tissue that were collected as part of standard clinical care between 1998 and 2012. In 15 of these cases, we collected additional samples including multiple brain metastasis lesions (7 cases) and extracranial lesions (8 cases with regional lymph node metastases, extracranial metastases, or additional primary-tumor tissue). All patients provided written informed consent for genetic analysis. Board-certified neuropathologists (S. Santagata, A. Stemmer-Rachamimov, and D.N. Louis) confirmed the histologic diagnoses and selected representative fresh-frozen or formalin-fixed

paraffin-embedded samples that had an estimated purity of ≥40%. We performed whole-exome sequencing of extracted tissue using methods as described on Illumina HiSeq or Genome Analyzer IIX platforms (48, 49). Samples were sequenced to median average depth of 108.3X (Supplementary Fig. S19). Of the 104 cases, we focused on the 86 (Supplementary Table S1) that exhibited sufficiently high purity in both the primary and brain-metastasis samples (16) and for which the DNA libraries were of sufficient quality (Supplementary Fig. S19 and Supplementary File S1). Somatic copy-number alterations were inferred from sequencing read depth (Supplementary Fig. S8, S9, S12–S18, S20, and Supplementary File S2). In addition, we performed deep targeted sequencing (median depth 455X) on a subset of primary-tumor samples using the Illumina HiSeq platform (50) to confirm the presence or absence of mutations (Supplementary Table S2). Immunohistochemistry for HER2/NEU overexpression was used to validate amplification of *ERBB2* in the brain metastasis and primary tumor in case 331.

Additional details regarding materials and methods are provided in the Supplementary Methods.

Accession codes: All data have been deposited in the database of Genotypes and Phenotypes (dbGaP): accession number phs000730.v1.p1.

Analysis codes: Source-code implementing methods used in this article can be accessed at http://bcb.dfci.harvard.edu/~scarter/clonalevolutionsuite.

Branched-Sibling Model

In order to address the genetic heterogeneity of cancer-tissue samples, we analyzed mutation CCF data to determine whether the tissue samples were sufficiently diverged from one another such that no detectable overlap of minor subclones (CCF < 1) occurred, a scenario we term the *branched-sibling* model (Supplementary Figs. S7B, S17A–S17C). In this model, the related cancer-tissue samples descend from a common ancestral clone, but each has continued to evolve independently with no overlap of subclones in the sampled tissues. In this scenario, it is valid to construct standard phylogenetic trees relating each tissue sample, with minor subclones (CCF < 1) private to each tissue sample represented as subtrees grafted on to each sample tip. The branched-sibling scenario implies that such trees accurately represent the evolutionary relationship of all subclonal populations detected with CCF = 1 in the sampled cancer tissues. A corollary of the branched-sibling model is that all mutations shared in two or more samples must have CCF = 1 wherever they are present. Thus, the appearance of mutations shared in two or more samples with CCF < 1 in any of them either represents technical artifact or constitutes evidence that the branched-sibling approximation is not an accurate description of those samples. Because some degree of technical artifact is occasionally expected, due to either sequencing errors or incorrect estimation of CCF values, we applied further logical constraints on the phylogenetic relationships between subclones in order to distinguish true violations of the branched-sibling scenario (described below).

To analyze the evolutionary relationship between paired primary-tumor and brain-metastasis samples, we first examined whether we could find any cell population in any primary-tumor sample that was an ancestor of the metastasis. Such a metastasis-founding subclone would harbor mutations in a subset of the cancer cells of the primary-tumor sample ($CCF_{primary} < 1$) that were present in all cancer cells ($CCF_{met} = 1$) of the metastasis sample (violating the branched-sibling model; Supplementary Fig. S7C). For each patient, we analyzed the two-dimensional CCF distributions of point mutations for all unique tissue-sample pairs (Supplementary Figs. S1 and S3 and Supplementary File S3) using a previously described 2-D Bayesian clustering algorithm (ref. 19; Supplementary Methods). In most patients, we observed some mutations with $CCF_{met} = 1$ that were not detected in the primary. Similarly, in most patients, we observed some mutations with $CCF_{primary} = 1$ that were not detected in the paired metastasis. We reasoned that, because subclones defined by $CCF_{primary} < 1$ and $CCF_{met} = 1$ must be the evolutionary siblings of subclones defined by $CCF_{primary} < 1$ and $CCF_{met} = 0$, a metastasis-founding subclone could not have been present at a detectable fraction in these primary-tumor samples, as this subclone would have displaced the mutations exclusive to the primary, so that none would have $CCF_{primary} = 1$ (Supplementary Fig. S7B). Thus, the observation of mutation clusters with $CCF_{primary} < 1$ and $CCF_{met} = 1$ in the absence of this displacement was not considered to be convincing evidence for a branched-sibling violation (Supplementary File S3). We recently applied similar analysis to data from a mouse model of lung cancer (20), where a valid metastasis-founding subclone was detected (Fig. 5 therein); however, we note that approximately 50% of the total tumor mass was harvested for sequencing in that case.

Following similar reasoning, we examined CCF values in all pairs of related cancer tissue samples. Most sample-pairs exhibited robust mutation clusters with CCF = 1 in one sample that were undetected in the other (Supplementary File S3), implying that they were sufficiently diverged from one another such that no partial-sharing of subclones occurred between them. We note that evidence supporting partial sharing of subclones between multiple sequenced regions of individual brain metastases was observed for some cases, necessitating special treatment (described below).

Phylogenetic Inference on Related Cancer-Tissue Samples

We created phylogenetic trees using a four-phase process in order to (i) be robust to both false-positive and false-negative mutation calls; (ii) assign mutations to the correct branches of the tree; (iii) distinguish tissue-restricted minor subclones, present in only a subset of the cancer cells in a given sample (CCF < 1); and (iv) identify cases where minor subclones were shared by two or more related tissue samples (violating the branched-sibling model) and correct the phylogenetic trees accordingly.

In the first phase, we sought to find the best phylogenetic tree explaining the observed point-mutation data. Somatic point-mutations were assumed to have arisen uniquely during the clonal evolution of the cancer, with negligible back-mutation rates, for example, due to chromosomal deletion of mutated alleles, which did not appear to help explain the data (not shown). We constructed a binary matrix of present/absent values for all point mutations detected in any of the samples analyzed from a given patient. For each sample, absent sites for which paired-detection power was <0.7 were removed from consideration, as were sites for which <3 reads supporting the mutation were observed. We then searched for the maximum-parsimony phylogeny using the parsimony-ratchet method (51) on this matrix.

In the second phase, we sought to assign mutations to branches of the phylogeny inferred in phase I, taking into account uncertainty in the provisional mutation forced calls. We applied the Bayesian clustering procedure described in the Supplementary Methods to each sample individually, retaining all mutations provisionally called with >0 supporting reads in that sample. A single pseudo-count observation was added having CCF = 1. We then identified all provisional mutation calls (>0 supporting reads) made in at least two samples of the case that were assigned to a CCF cluster with posterior mode < 1.0 (Supplementary Fig. S5A). These mutation calls, which appeared to violate the branched-sibling model (described above), were then rejected if the number of supporting reads was <3 (Supplementary Fig. S5B). This modified matrix of mutation calls was then used to assign each mutation to a branch of the phylogenetic tree by assuming that the mutation occurred uniquely during clonal evolution and was not subject to back mutation. For each sample, the number of mutations in each category is shown in Supplementary Fig. S5C. Assignment of gene-level SCNAs to branches was performed in a similar manner (Supplementary Fig. S5D).

In the third phase, we sought to obtain a more complete description of the genetic divergence between the various tissue samples of

each case. We refined the tips of each phylogenetic tree by distinguishing between private mutations that occurred in all cancer cells of each sample (CCF = 1) versus those that occurred in a restricted subset of sampled cancer cells (CCF < 1). To make this distinction, for each sample, we applied the Bayesian clustering technique (described in Supplementary Methods) to the private mutations called only in that sample. We added *N* pseudo-count observations of CCF = 1, where *N* was the number of mutations called in >1 samples of the case that were also called in the sample being considered. This process partitioned the private mutations into a small number of putative subclones having distinct CCF values (Supplementary Fig. S4). We then modified the phylogenetic trees by replacing each (non-germline) tip with a subtree representing the maximally branching microphylogeny consistent with the observed set of CCF-cluster values (i.e., respecting the rule that the sum of sibling subclones cannot exceed that of their most recent common ancestor; Figs. 1, 3, and 4, and Supplementary Fig. S6).

In the fourth phase, we examined whether evidence that the branched-sibling model was not an adequate approximation of the sampled cancer tissues could be discerned. We manually reviewed detailed plots (Supplementary File S3) showing the estimated CCF value of each mutation in each tissue sample, as well as the 2-D clustering results of mutation CCF values in all unique pairs of related tissue samples (Supplementary Fig. S3) for evidence of minor subclones (CCF < 1) shared by two or more samples, as described above. In two cases in which evidence contradicting the branched-sibling model was observed, phylogenetic trees were manually adjusted (as described below) to accurately reflect the evolutionary relationship between the different clonal lineages as shown in Fig. 3C and F. This was done in a manner analogous to that described in a recent report (20); here, we extended similar logic to the scenario where the same subclone was present in multiple sequenced tissue samples. Detailed analysis of mutation CCFs for each patient, including the automatically generated phylogenetic trees (prior to manual adjustment), are available in Supplementary File S3.

For patient 138 (Fig. 3F), samples BM1 region1 and BM1 region2 shared a minor subclone (subclone1) defined by 15 mutations, present at CCF = 0.6 in BM1 region 1 and CCF = 0.55 in BM1 region 2. Because the mutations private to these samples had CCF values consistent with being the siblings of subclone1 (CCF = 0.1 in BM1 region 1 and CCF = 0.3 in BM1 region2), we redrew the tree this way.

For patient 314 (Fig. 3C), samples BM region 2 and BM region 4 shared a minor subclone (subclone 2) defined by eight mutations, present at CCF = 0.45 in BM region 2 and CCF = 0.35 in BM region 4. Samples BM region 1 and BM region 3 shared a minor subclone (subclone 1), defined by seven mutations, present at CCF = 0.55 in BM region 3 and CCF = 0.4 in BM region 1. In addition, BM region 1 and BM region 3 appeared to contain a small number of cells (CCF < 0.05) from subclone 2. In addition, extreme heterogeneity of primary-tumor sample may have resulted in inaccurate CCF values for some mutations, leading to the appearance of a cluster having CCF < 1 in the primary and CCF = 1 in all metastasis samples.

Patients 176, 302, and 137 showed some evidence consistent with shared subclones, but due to the small number of mutations involved and the uncertainty in their CCF values, judgments about the validity of these branched-sibling violations could not be made with confidence. The trees were therefore left unaltered.

In addition, patients 331, 104, 52, 263, and 91 harbored shared mutations with CCF < 1. However, they were not logically consistent with true violations of the branched-sibling model (e.g., they failed to displace private mutations, which were present at CCF = 1 in most samples from these cases). This, coupled with the substantial heterogeneity of the copy profiles in some of these samples, led us to conclude that the appearance of mutations appearing to violate the branched-sibling model was due to incorrect estimation of CCF values.

Prioritization of Clinically Informative Mutations Using TARGET

To systematically evaluate somatic alterations of potential clinical interest, we used the TARGET database (31) of genes for which somatic alterations have therapeutic or prognostic implications in at least one tumor type (Supplementary Table S3). Because the therapeutic or prognostic evidence in TARGET is often based on one or a few tumor types, we currently do not have evidence that these events will be predictive of clinical responses to the indicated targeted therapeutic agent in all of the tumor types studied here. Ongoing clinical trials to test such hypotheses ("basket trials") accept any patient with a particular alteration regardless of their primary histology. However, there is evidence that in some cases, such as for BRAF V600E mutations in colorectal cancer, the responses to therapies targeting the same genomic events are histology dependent.

Alterations in TARGET genes were prioritized according to defined criteria (31). For example, some genes were required to have biallelic inactivation, whereas others required amplification or specific point mutations. In order to nominate a mutation as "potentially clinically informative," we first distinguished between heterozygous and homozygous events (in which no reference alleles remained in the cancer cells), by analyzing read-counts at mutated loci using ABSOLUTE (16) to account for genomic copy numbers and sample purity.

We accepted as fulfilling the "biallelic inactivation" TARGET criteria genes harboring homozygous loss-of-function (LOF) mutations, homozygous deletion, or two heterozygous LOF mutations. LOF mutations were defined as: nonsense, frame-shift indel, in-frame indel, or splice site mutations. To satisfy the "mutation" TARGET criteria, we required the presence of at least one identical amino acid substitution in the Catalogue of Somatic Mutations in Cancer (COSMIC) database (v67; ref. 52). To satisfy the "amplification" TARGET criteria, we required a gene-level somatic copy-number alteration call of either "amplification" or "high-level amplification" (as described above).

Disclosure of Potential Conflicts of Interest

E.M. Van Allen is a consultant/advisory board member for Syapse and Roche Ventana. B.E. Johnson has ownership interest (including patents) in KEW Group and is a consultant/advisory board member for the same. M. Meyerson reports receiving a commercial research grant from Bayer; has ownership interest in Foundation Medicine and in a patent licensed to Laboratory Corporation of America; and is a consultant/advisory board member for Foundation Medicine. L.A. Garraway reports receiving a commercial research grant from Novartis; has ownership interest (including patents) in Foundation Medicine; and is a consultant/advisory board member for Novartis, Foundation Medicine, Boehringer Ingelheim, and Warp Drive. R. Beroukhim is a consultant at Novartis and reports receiving a commercial research grant from Novartis. T. Batchelor reports receiving a commercial research grant from Pfizer; has received speakers bureau honoraria from Research To Practice, Imedex, and Oakstone; and is a consultant/advisory board member for Proximagen, Merck, Foundation Medicine, UpToDate, and Champions Biotechnology. W.C. Hahn reports receiving a commercial research grant from Novartis and is a consultant/advisory board member for the same. No potential conflicts of interest were disclosed by the other authors.

One of the Editors-in-Chief is an author on this article. In keeping with the AACR's editorial policy, the peer review of this submission was managed by a senior member of *Cancer Discovery*'s editorial team; a member of the AACR Publications Committee rendered the final decision concerning acceptability.

Authors' Contributions

Conception and design: P.K. Brastianos, S.L. Carter, S. Santagata, T.T. Batchelor, J. Baselga, D.N. Louis, G. Getz, W.C. Hahn

Development of methodology: P.K. Brastianos, S.L. Carter, S. Santagata, T.T. Batchelor, J. Baselga, D.N. Louis, G. Getz, W.C. Hahn

Acquisition of data (provided animals, acquired and managed patients, provided facilities, etc.): P.K. Brastianos, S. Santagata, D.P. Cahill, R.T. Jones, P.M. Horowitz, J. Tabernero, J. Seoane, E. Martinez-Saez, W.T. Curry, I.F. Dunn, S.H. Paek, S.-H. Park, F.G. Barker II, C.M. Gill, B.E. Johnson, T.K. Choueiri, S. Signoretti, C. Sougnez, M.S. Rabin, N.U. Lin, E.P. Winer, A. Stemmer-Rachamimov, D.N. Louis

Analysis and interpretation of data (e.g., statistical analysis, biostatistics, computational analysis): P.K. Brastianos, S.L. Carter, A. Taylor-Weiner, E.M. Van Allen, M.S. Lawrence, P.M. Horowitz, K. Cibulskis, A. McKenna, A. Chevalier, M. Rosenberg, J. Baselga, D.N. Louis, G. Getz, W.C. Hahn

Writing, review, and/or revision of the manuscript: P.K. Brastianos, S.L. Carter, T.T. Batchelor, J. Baselga, D.N. Louis, G. Getz, W.C. Hahn

Administrative, technical, or material support (i.e., reporting or organizing data, constructing databases): P.K. Brastianos

Other (pathology review): S. Santagata, A. Stemmer-Rachamimov, D.N. Louis

Other (obtaining institutional review board approval): P.K. Brastianos

Other (coordinating and performing exome sequencing): P.K. Brastianos, S. Santagata, R.T. Jones, C. Sougnez

Other (managing tissue repositories at Dana-Farber and MGH): K.L. Ligon, A. Stemmer-Rachamimov, D.N. Louis

Other (supervising sequencing platform at Dana-Farber Cancer Institute): P. Van Hummelen, A.R. Thorner

Other (immunohistochemistry staining): M.P. Hoang

Other (providing fruitful discussions about the interpretation of results): M. Meyerson, L. Garraway

Acknowledgments

This article is dedicated to Maria Brastianos. The authors would like to thank the patients for providing tissue samples; Loreal Brown, James Kim, and Bill Richards for assisting with sample collection; Anna Schinzel and Gary Ciocci for fruitful discussions; Leslie Gaffney for assisting with the figures, and Charilaos H. Brastianos for critical review of the manuscript.

Grant Support

This work was supported a grant from the NIH (National Human Genome Research Institutes of Health Large-Scale Sequencing and Analysis Center) U54 HG003067 (to E.S. Lander) to the Broad Institute; the National Cancer Institute (TCGA Genome Characterization Center) 5U24CA143687 (to M. Meyerson and S. Gabriel) to the Broad Institute; the Brain Science Foundation (to P.K. Brastianos); Susan G. Komen for the Cure (to P.K. Brastianos); Terri Brodeur Breast Cancer Foundation (to P.K. Brastianos); Conquer Cancer Foundation (to P.K. Brastianos); the American Brain Tumor Association (to P.K. Brastianos); the Breast Cancer Research Foundation (to P.K. Brastianos); U54CA143798 (to R. Beroukhim and P.K. Brastianos); and the Mary Kay Foundation (to P.K. Brastianos and W.C. Hahn). W.C. Hahn and R. Beroukhim are supported by Novartis. G. Getz is the Paul C. Zamecnick, MD, Chair in Oncology at MGH. N.U. Lin and E.P. Winer are supported by the Breast Cancer Research Foundation.

Received March 30, 2015; revised August 8, 2015; accepted August 11, 2015; published OnlineFirst September 26, 2015.

REFERENCES

1. Brastianos PK, Curry WT, Oh KS. Clinical discussion and review of the management of brain metastases. J Natl Compr Canc Netw 2013; 11:1153–64.
2. Eichler AF, Chung E, Kodack DP, Loeffler JS, Fukumura D, Jain RK. The biology of brain metastases-translation to new therapies. Nat Rev Clin Oncol 2011;8:344–56.
3. Campbell PJ, Yachida S, Mudie LJ, Stephens PJ, Pleasance ED, Stebbings LA, et al. The patterns and dynamics of genomic instability in metastatic pancreatic cancer. Nature 2010;467:1109–13.
4. Gerlinger M, Rowan AJ, Horswell S, Larkin J, Endesfelder D, Gronroos E, et al. Intratumor heterogeneity and branched evolution revealed by multiregion sequencing. N Engl J Med 2012;366:883–92.
5. Liu W, Laitinen S, Khan S, Vihinen M, Kowalski J, Yu G, et al. Copy number analysis indicates monoclonal origin of lethal metastatic prostate cancer. Nat Med 2009;15:559–65.
6. Navin N, Kendall J, Troge J, Andrews P, Rodgers L, McIndoo J, et al. Tumour evolution inferred by single-cell sequencing. Nature 2011;472:90–4.
7. Ding L, Ellis MJ, Li S, Larson DE, Chen K, Wallis JW, et al. Genome remodelling in a basal-like breast cancer metastasis and xenograft. Nature 2010;464:999–1005.
8. Xie T, Cho YB, Wang K, Huang D, Hong HK, Choi YL, et al. Patterns of somatic alterations between matched primary and metastatic colorectal tumors characterized by whole-genome sequencing. Genomics 2014;104:234–41.
9. Shah SP, Morin RD, Khattra J, Prentice L, Pugh T, Burleigh A, et al. Mutational evolution in a lobular breast tumour profiled at single nucleotide resolution. Nature 2009;461:809–13.
10. Paik PK, Shen R, Won H, Rekhtman N, Wang L, Sima CS, et al. Next-generation sequencing of stage IV squamous cell lung cancers reveals an association of PI3K aberrations and evidence of clonal heterogeneity in patients with brain metastases. Cancer Discov 2015;5:610–21.
11. Chen G, Chakravarti N, Aardalen K, Lazar AJ, Tetzlaff MT, Wubbenhorst B, et al. Molecular profiling of patient-matched brain and extracranial melanoma metastases implicates the PI3K pathway as a therapeutic target. Clin Cancer Res 2014;20:5537–46.
12. Wikman H, Lamszus K, Detels N, Uslar L, Wrage M, Benner C, et al. Relevance of PTEN loss in brain metastasis formation in breast cancer patients. Breast Cancer Res 2012;14:R49.
13. Bos PD, Zhang XH, Nadal C, Shu W, Gomis RR, Nguyen DX, et al. Genes that mediate breast cancer metastasis to the brain. Nature 2009;459:1005–9.
14. McMullin RP, Wittner BS, Yang C, Denton-Schneider BR, Hicks D, Singavarapu R, et al. A BRCA1 deficient-like signature is enriched in breast cancer brain metastases and predicts DNA damage-induced poly (ADP-ribose) polymerase inhibitor sensitivity. Breast Cancer Res 2014;16:R25.
15. Haffner MC, Mosbruger T, Esopi DM, Fedor H, Heaphy CM, Walker DA, et al. Tracking the clonal origin of lethal prostate cancer. J Clin Invest 2013;123:4918–22.
16. Carter SL, Cibulskis K, Helman E, McKenna A, Shen H, Zack T, et al. Absolute quantification of somatic DNA alterations in human cancer. Nat Biotechnol 2012;30:413–21.
17. Nik-Zainal S, Alexandrov LB, Wedge DC, Van Loo P, Greenman CD, Raine K, et al. Mutational processes molding the genomes of 21 breast cancers. Cell 2012;149:979–93.
18. Landau DA, Carter SL, Getz G, Wu CJ. Clonal evolution in hematological malignancies and therapeutic implications. Leukemia 2014;28:34–43.
19. Landau DA, Carter SL, Stojanov P, McKenna A, Stevenson K, Lawrence MS, et al. Evolution and impact of subclonal mutations in chronic lymphocytic leukemia. Cell 2013;152:714–26.
20. McFadden DG, Papagiannakopoulos T, Taylor-Weiner A, Stewart C, Carter SL, Cibulskis K, et al. Genetic and clonal dissection of murine small cell lung carcinoma progression by genome sequencing. Cell 2014;156:1298–311.
21. Lohr JG, Stojanov P, Carter SL, Cruz-Gordillo P, Lawrence MS, Auclair D, et al. Widespread genetic heterogeneity in multiple myeloma: implications for targeted therapy. Cancer Cell 2014;25:91–101.
22. Yachida S, Jones S, Bozic I, Antal T, Leary R, Fu B, et al. Distant metastasis occurs late during the genetic evolution of pancreatic cancer. Nature 2010;467:1114–7.
23. Ihle NT, Lemos R, Wipf P, Yacoub A, Mitchell C, Siwak D, et al. Mutations in the phosphatidylinositol-3-kinase pathway predict for antitumor activity of the inhibitor PX-866 whereas oncogenic Ras is a dominant predictor for resistance. Cancer Res 2009;69:143–50.
24. Sos ML, Koker M, Weir BA, Heynck S, Rabinovsky R, Zander T, et al. PTEN loss contributes to erlotinib resistance in EGFR-mutant

lung cancer by activation of Akt and EGFR. Cancer Res 2009;69: 3256–61.
25. Juric D, Castel P, Griffith M, Griffith OL, Won HH, Ellis H, et al. Convergent loss of PTEN leads to clinical resistance to a PI(3)Kalpha inhibitor. Nature 2015;518:240–4.
26. Lynch TJ, Bell DW, Sordella R, Gurubhagavatula S, Okimoto RA, Brannigan BW, et al. Activating mutations in the epidermal growth factor receptor underlying responsiveness of non-small-cell lung cancer to gefitinib. N Engl J Med 2004;350:2129–39.
27. Krop I, Flores L, Najita JS, Mayer IA, Hobday TJ, Falkson I, et al. The role of EGFR amplification in trastuzumab resistance: a correlative analysis of TBCRC003. J Clin Oncol 29: 2011 (suppl; abstr 528.
28. Ritter CA, Perez-Torres M, Rinehart C, Guix M, Dugger T, Engelman JA, et al. Human breast cancer cells selected for resistance to trastuzumab in vivo overexpress epidermal growth factor receptor and ErbB ligands and remain dependent on the ErbB receptor network. Clin Cancer Res 2007;13:4909–19.
29. TCGA. Integrated genomic analyses of ovarian carcinoma. Nature 2011;474:609–15.
30. Bang YJ, Van Cutsem E, Feyereislova A, Chung HC, Shen L, Sawaki A, et al. Trastuzumab in combination with chemotherapy versus chemotherapy alone for treatment of HER2-positive advanced gastric or gastro-oesophageal junction cancer (ToGA): a phase 3, open-label, randomised controlled trial. Lancet 2010;376:687–97.
31. Van Allen EM, Wagle N, Stojanov P, Perrin DL, Cibulskis K, Marlow S, et al. Whole-exome sequencing and clinical interpretation of formalin-fixed, paraffin-embedded tumor samples to guide precision cancer medicine. Nat Med 2014;20:682–8.
32. Finn RS, Dering J, Conklin D, Kalous O, Cohen DJ, Desai AJ, et al. PD 0332991, a selective cyclin D kinase 4/6 inhibitor, preferentially inhibits proliferation of luminal estrogen receptor-positive human breast cancer cell lines in vitro. Breast Cancer Res 2009;11:R77.
33. Logan JE, Mostofizadeh N, Desai AJ, VON Euw E, Conklin D, Konkankit V, et al. PD-0332991, a potent and selective inhibitor of cyclin-dependent kinase 4/6, demonstrates inhibition of proliferation in renal cell carcinoma at nanomolar concentrations and molecular markers predict for sensitivity. Anticancer Res 2013;33:2997–3004.
34. Booher RN, Hatch H, Dolinski BM, Nguyen T, Harmonay L, Al-Assaad AS, et al. MCL1 and BCL-xL levels in solid tumors are predictive of dinaciclib-induced apoptosis. PLoS ONE 2014;9:e108371.
35. Fry DW, Harvey PJ, Keller PR, Elliott WL, Meade M, Trachet E, et al. Specific inhibition of cyclin-dependent kinase 4/6 by PD 0332991 and associated antitumor activity in human tumor xenografts. Mol Cancer Ther 2004;3:1427–38.
36. Cancer Genome Atlas Research Network. Comprehensive genomic characterization defines human glioblastoma genes and core pathways. Nature 2008;455:1061–8.
37. Jaiswal BS, Janakiraman V, Kljavin NM, Chaudhuri S, Stern HM, Wang W, et al. Somatic mutations in p85alpha promote tumorigenesis through class IA PI3K activation. Cancer Cell 2009;16:463–74.
38. Bose R, Kavuri SM, Searleman AC, Shen W, Shen D, Koboldt DC, et al. Activating HER2 mutations in HER2 gene amplification negative breast cancer. Cancer Discov 2013;3:224–37.
39. Engelman JA, Chen L, Tan X, Crosby K, Guimaraes AR, Upadhyay R, et al. Effective use of PI3K and MEK inhibitors to treat mutant Kras G12D and PIK3CA H1047R murine lung cancers. Nat Med 2008; 14:1351–6.
40. Wada M, Horinaka M, Yamazaki T, Katoh N, Sakai T. The dual RAF/MEK inhibitor CH5126766/RO5126766 may be a potential therapy for RAS-mutated tumor cells. PLoS ONE 2014;9:e113217.
41. Kikuchi J, Takashina T, Kinoshita I, Kikuchi E, Shimizu Y, Sakakibara-Konishi J, et al. Epigenetic therapy with 3-deazaneplanocin A, an inhibitor of the histone methyltransferase EZH2, inhibits growth of non-small cell lung cancer cells. Lung Cancer 2012;78:138–43.
42. Rochet NM, Dronca RS, Kottschade LA, Chavan RN, Gorman B, Gilbertson JR, et al. Melanoma brain metastases and vemurafenib: need for further investigation. Mayo Clin Proc 2012;87:976–81.
43. Maillet D, Martel-Lafay I, Arpin D, Perol M. Ineffectiveness of crizotinib on brain metastases in two cases of lung adenocarcinoma with EML4-ALK rearrangement. J Thorac Oncol 2013;8:e30–1.
44. Musolino A, Ciccolallo L, Panebianco M, Fontana E, Zanoni D, Bozzetti C, et al. Multifactorial central nervous system recurrence susceptibility in patients with HER2-positive breast cancer: epidemiological and clinical data from a population-based cancer registry study. Cancer 2011;117:1837–46.
45. Patchell RA, Tibbs PA, Walsh JW, Dempsey RJ, Maruyama Y, Kryscio RJ, et al. A randomized trial of surgery in the treatment of single metastases to the brain. N Engl J Med 1990;322:494–500.
46. Stortebecker TP. Metastatic tumors of the brain from a neurosurgical point of view; a follow-up study of 158 cases. J Neurosurg 1954;11: 84–111.
47. Patchell RA, Tibbs PA, Regine WF, Dempsey RJ, Mohiuddin M, Kryscio RJ, et al. Postoperative radiotherapy in the treatment of single metastases to the brain: a randomized trial. JAMA 1998;280: 1485–9.
48. Brastianos PK, Horowitz PM, Santagata S, Jones RT, McKenna A, Getz G, et al. Genomic sequencing of meningiomas identifies oncogenic SMO and AKT1 mutations. Nat Genet 2013;45:285–9.
49. DePristo MA, Banks E, Poplin R, Garimella KV, Maguire JR, Hartl C, et al. A framework for variation discovery and genotyping using next-generation DNA sequencing data. Nat Genet 2011;43:491–8.
50. Hong YS, Kim J, Pectasides E, Fox C, Hong SW, Ma Q, et al. Src Mutation induces acquired lapatinib resistance in ERBB2-amplified human gastroesophageal adenocarcinoma models. PLoS ONE 2014;9:e109440.
51. Nixon KC. The parsimony ratchet, a new method for rapid parsimony analysis. Cladistics 1999;15:407–14.
52. Shepherd R, Forbes SA, Beare D, Bamford S, Cole CG, Ward S, et al. Data mining using the catalogue of somatic mutations in cancer BioMart. Database 2011;2011:bar018.